Effects of Quasi-Nanogel Particles on the Rheological and Mechanical Properties of Natural Rubber: A New Insight

Suman Mitra, Santanu Chattopadhyay, Anil K. Bhowmick

Rubber Technology Centre, Indian Institute of Technology, Kharagpur 721302, India

Received 25 March 2007; accepted 25 June 2007
DOI 10.1002/app.26962
Published online 13 November 2007 in Wiley InterScience (www.interscience.wiley.com).

ABSTRACT: The influence of sulfur-crosslinked, quasi-nanosized gels on the rheological and mechanical properties of raw natural rubber (NR) was investigated. Latex gels with different crosslink densities were prepared through the variation of the sulfur-to-accelerator ratio. These gels were characterized by dynamic light scattering, solvent swelling, and mechanical properties. The gels were mixed with raw NR latex at concentrations of 2, 4, 8, and 16 phr, and their effect on the rheological properties of NR was studied by Monsanto processability tester. The presence of gel in raw NR reduced the apparent shear viscosity and die swell considerably. Initially, the viscosity decreased up to a 8 phr gel loading and then increased with an increase in the gel loading. However, the change in the viscosity was related to the crosslink density of the gels. A new empirical equation relating the viscosity, volume fraction of the gels, and crosslink density was proposed. The die swell of gel-filled raw NR was at least 10% lower than that of unfilled raw NR and decreased with an increase in the gel loading. The effect of the gels on the die swell properties was explained through the calculation of the principal normal stress difference of gel-filled NR systems. Scanning electron photomicrographs of the extrudates revealed much better surface smoothness for the gel-filled virgin rubber systems than for the unfilled rubber. The addition of the gels to raw NR increased the modulus and tensile strength, whereas the elongation at break decreased. The effect of the gels on the dynamic mechanical properties of NR was also investigated. J Appl Polym Sci 107: 2755–2767, 2008

Key words: gels; latices; mechanical properties; rheology; rubber; viscosity

INTRODUCTION

The processing behavior of an elastomer plays a key role during various stages of product manufacturing operations such as mixing, extrusion, calendering, and molding. The flow behavior of raw, unfilled elastomers at given temperatures and shear rates is a major aspect of any processing step. The prediction of the performance and the control of a particular processing step require knowledge of both the viscous and the elastic properties of a polymer compound. The viscous flow is linked to the output rate, whereas the elastic behavior governs the dimensional stability. The knowledge of both these parameters for a particular compound is important in understanding its processing behavior. Many researchers have studied the effect of crosslinked particles (gels) on virgin polymer matrices with respect to their rheological properties. Extensive work has been done in this area with plastic matrices in particular. The surface effect of crosslinked poly(methyl methacrylate) on the rheological properties of polystyrene has been studied extensively.[1,2] In a similar study, the influence of core–shell particles on a viscoelastic poly(methyl methacrylate) matrix has been investigated in detail.[3] Some researchers have also studied the effects of the particle size, volume fraction, and surface treatment of crosslinked polystyrene particles on various properties of crosslinked natural rubber (NR).[4,5] In the rubber industry, gels are added to rubber to improve the processability of rubber and rubber compounds to a great extent. The advantages of such a procedure are well documented in the literature.[6] Several researchers have reported the effects of gels on raw rubber. The flow characteristics of raw nitrile rubber containing divinyl benzene crosslinked gel particles were investigated by Nakajima and Collins.[7] Montes and Ponce-Velez[8] reported the effects of gels on the extrusion behavior of guayule rubber. The viscosity increased upon the incorporation of the gels, and this was more evident at lower shear rates. Bhowmick et al.[9] studied the influence of gels on the crystallization, stress relaxation, and orientation properties of NR. Campbell and Fuller[10] observed that a gel produces a slight decrease in the rate of relaxation of raw NR. The effect of a gel on the green strength of NR has also been reported in the literature.[11] Understanding the effects of various types of gels on the raw rubber performance and especially

Correspondence to: A. K. Bhowmick (anilkb@rtc.iitkgp.ernet.in).

Contract grant sponsor: Department of Atomic Energy (DAE), Board of Research in Nuclear Sciences (BRNS); contract grant number: 2005/35/4/BRNS/516.

Journal of Applied Polymer Science, Vol. 107, 2755–2767 (2008)

on the rheological properties is of tremendous commercial importance because it could lead to the introduction of even better processing grades of rubber than the existing ones. Despite a few studies conducted earlier, the exact nature of the influence of gels on the properties of raw rubber has not been elucidated systematically in terms of the gel size, shape, and degree of crosslinking to date. Moreover, conventional rheological studies of raw polymers are conducted with fillers or particulate inclusions that are very rigid with moduli in the range of a few gigapascals.[12] Extensive research work has not been carried out to determine the effects of semirigid or deformable particles having gradients of rigidity and crosslinking density on the viscosity of raw polymers. It would be especially interesting if the gels had nanosized or nearly nanosized (quasi-nanosized) dimensions. It has been reported by our laboratory that nanoparticles exhibit unique mechanical and rheological behavior.[13,14] On the other hand, the improvement of various properties upon the incorporation of gels shows different trends for different rubbers and is largely dependent on both the type of the gel and the respective elastomers in which the gel is incorporated. Hence, further investigations are necessary in this area. In this work, we attempted to elucidate the rheological implications of quasi-nanosized ($\sim$ 100–300 nm) deformable gels on a raw NR matrix by varying the nature of the gel particles. An NR latex was crosslinked with sulfur at five different sulfur-to-accelerator ratios to form a crosslinked gelled latex. These gels were thoroughly characterized, then mixed with raw NR latex at concentrations of 2, 4, 8, and 16 phr in the latex stage, and finally air-dried. Their effect on the raw NR properties, with reference to capillary rheometry in particular, was investigated in detail.

EXPERIMENTAL

Materials

High-ammonia-centrifuged NR with a 60% dry rubber content (DRC) was generously supplied by the Rubber Board (Kottayam, India). Sulfur, zinc oxide (ZnO), and zinc diethyl dithiocarbamate (ZDC), all in 50% aqueous dispersions, were obtained from the same source and used as received. Potassium hydroxide (KOH) and potassium laurate ($KC_{12}H_{23}O_2$) were supplied by S.D. Fine Chemicals (Mumbai, India). All other chemicals (Laboratory Reagent-grade) and deionized water were obtained from indigenous sources.

Preparation of the sulfur-prevulcanized latex gel and gel-filled rubber

The formulations of the different mixes for sulfur prevulcanization are given in Table I. The prevulcanization of the compounded latex was carried out at 80°C for 2 h with a water bath with constant gentle stirring in a round-bottom flask fitted with a condenser.[15] Films were prepared through casting onto a glass plate and dried at the ambient temperature. The dried films were leached in 1% ammoniacal water for 24 h and dried in air again until they were transparent. Finally, the latex films were heated in a vacuum oven at 50°C for 2 h. These were used for the characterization of gelled rubber.

TABLE I
Formulation of the Mixes for the Sulfur-Prevulcanized Latex Gels

Ingredient (dry weight basis)	$NS_{0.33}$	$NS_{0.5}$	NS_1	NS_2	NS_3
NR latex (60%)	100.00	100.00	100.00	100.00	100.00
10% KOH	0.25	0.25	0.25	0.25	0.25
10% $KC_{12}H_{23}O_2$	0.25	0.25	0.25	0.25	0.25
50% sulfur dispersion	0.60	0.60	1.20	1.20	1.80
50% ZDC dispersion	1.80	1.20	1.20	0.60	0.60
50% ZnO dispersion	0.20	0.20	0.20	0.20	0.20

Gel-mixed rubber samples were prepared by the addition of the prevulcanized NR latex to the raw NR latex in different concentrations and stirred at a slow speed for 1 h. Then, they were cast and dried according to the aforementioned procedure.

Sample designations

The sulfur-prevulcanized latex gel-mixed raw NR systems are designated $NS_{a/b}$, where a is the ratio of sulfur to the accelerator and b is the concentration (phr) of the sulfur-prevulcanized gel added to the raw NR latex. $NS_{1/8}$ represents a system in which a sulfur-prevulcanized latex gel with a sulfur-to-accelerator ratio of 1, at a concentration of 8 phr, was added to the raw NR latex. Likewise, $NS_{0.5/16}$ means that a sulfur-prevulcanized gel with a sulfur-to-accelerator ratio of 0.50 was added to raw NR at a concentration of 16 phr.

The gels are designated NS_a; for example, NS_2 denotes a sulfur-prevulcanized gel with a sulfur-to-accelerator ratio of 2. The control raw NR sample is denoted N_0.

Characterization of the gelled latex samples

Gel content

The gel fraction of the prevulcanized latex gels was measured through the immersion of the samples in toluene at room temperature (25 ± 1°C) for 48 h (the equilibrium swelling time, which was determined from the experiments) and calculated from the

weights of the samples before and after swelling as follows:

$$\text{Gel fraction} = W_2/W_1 \quad (1)$$

where W_1 is the initial weight of the polymer and W_2 is the weight of the insoluble portion of the polymer. The reported results are the averages of three samples.

Determination of the crosslink density

The crosslink density, which is the number of network chains per unit of volume, was determined from the initial weight, swollen weight, and final deswollen weight of the samples. The samples were swollen in toluene. The number of crosslink points (ν) per unit of volume was calculated from the following equation:[16]

$$\nu = \frac{-1}{V}\left[\frac{\ln(1-\upsilon_r)+\upsilon_r+\chi_1\upsilon_r^2}{\upsilon_r^{\frac{1}{3}}-\frac{\upsilon_r}{2}}\right] \quad (2)$$

where χ_1 is the polymer–solvent interaction parameter, V is the molar volume of the solvent, and υ_r is the volume fraction of the rubber in the swollen gel. υ_r was calculated from the following equation:[17]

$$\upsilon_r = \frac{(D_S - F_f A_w)\rho_r^{-1}}{(D_S - F_f A_w)\rho_r^{-1} + A_s\rho_s^{-1}} \quad (3)$$

where D_s, F_f, A_w, A_s, ρ_r, and ρ_s are the deswollen weight of the sample, insoluble fraction, sample weight, weight of the absorbed solvent corrected for the swelling increment, density of the rubber, and density of the solvent, respectively.

Dynamic light scattering (DLS) study

For the measurements of the particle size and distribution by the DLS method, latex samples were diluted to a 0.1 g/L concentration level with doubly distilled water, which was filtered through a Millipore (Bangalore, India) Millex syringe filter (Triton-free, 0.22 μm). The DLS studies were carried out with a Zetasizer Nano-ZS (Malvern Instrument, Ltd., Worcestershire, United Kingdom). The data were analyzed with in-built machine software.

Tensile testing

Tensile specimens were punched from cast sheets with ASTM Die-C. The tests were carried out according to the ASTM D 412-98 method in a universal testing machine (Z010, Zwick Roell, Ulm, Germany) at a crosshead speed of 500 mm/min at 25 ± 1°C. The average of three tests is reported here. TestXpert II software (Zwick Roell Ulm, Germany) was used for data acquisition and analysis. The same procedure was followed for the gel-filled raw NR samples.

Dynamic mechanical analysis

The dynamic mechanical properties of the gels and gel-filled raw NR were measured as a function of temperature with a DMA 2980 dynamic mechanical analyzer (TA Instruments, Newcastle, Delaware). The peak value of the tan δ curves was taken as the glass-transition temperature. The measurements were taken in the tension mode in the temperature range of −85 to 50°C at a heating rate of 3°C/min and at a frequency of 1 Hz. Thermal Advantage software (TA Instruments, Newcastle, Delaware) was used for the data acquisition and analysis.

Measurement of the rheological properties

The melt flow properties of the NR samples with and without gel were measured with a Monsanto processability tester (Monsanto Company, Akron, Ohio) (barrel radius = 9.53 mm), which is a fully automated capillary rheometer. The entire barrel and the capillary assembly were electrically heated with a microprocessor-based temperature controller. The capillary had a length-to-diameter ratio equal to 30 (length = 30.0 mm, diameter = 1.0 mm). The compound entrance angles of the capillary were 45 and 60°, which are known to minimize the pressure drop at the entrance. Therefore, the Bagley correction factor was assumed to be negligible, and the apparent shear stress (τ_{app}) was taken as equal to the true shear stress.[18] The preheating time for each sample was 5 min. The extrusion studies were carried out at 130°C at four different shear rates of 61.3, 122.5, 306.3, and 612.5 s^{-1}. The rate of shear variation was achieved through automatic changes in the speed of the plunger. The pressure at the entrance of the capillary was recorded automatically with the help of a pressure transducer. τ_{app}, the apparent shear rate ($\dot{\gamma}_{app}$), and the apparent shear viscosity (η_{app}) were calculated using standard equations[19] and according to an earlier report.[18]

The flow behavior index (n) and consistency index (k) were calculated with the power-law model:[19]

$$\tau_{app} = k\,\dot{\gamma}_{app}^{\,n} \quad (4)$$

By definition

$$\eta_{app} = \tau_{app}/\dot{\gamma}_{app} \quad (5)$$

Therefore

$$\eta_{app} = k\,\dot{\gamma}_{app}^{\,n-1} \quad (6)$$

The logarithmic form for eq. (6) can be written as follows:

$$\log \eta_{app} = \log k + (n-1) \log \dot{\gamma}_{app} \quad (7)$$

The values of n and k were calculated from the initial linear region observed at a lower shear rate.

Determination of the die swell

The die swell measurements were directly obtained from the Monsanto processability tester through a microprocessor-controlled laser beam assembly according to the following equation:

$$\text{Die swell} = \frac{d_e - d_c}{d_c} \times 100 \quad (8)$$

where d_e is the extrudate diameter and d_c is the capillary diameter.

Maximum recoverable deformation (γ_m)

γ_m was calculated with the following equations:[20]

$$\gamma_m = \sqrt{\frac{1}{2C}}(\alpha^{-4} + 2\alpha^2 - 3) \quad (9)$$

where

$$C = \frac{3\,n' + 1}{4(n' + 1)} \quad (10)$$

α is the extrudate swell, and n' is equal to n determined from the slope of log η_{app} versus log $\dot{\gamma}_{app}$ plots based on eq. (7).

Principal normal stress difference (σ_E)

σ_E in an elastic body was calculated with the following general equation:[21]

$$\sigma_E = \frac{(2 + \gamma_m)\gamma_m}{2(1 + \gamma_m)} (2\tau_{app}) \quad (11)$$

γ_m is a complex function of the filler loading, temperature, and nature of the fluid.

Calculation of the activation energy

The activation energy of viscous flow was calculated using the Arrhenious–Frenkel–Eyring equation,[21] which is valid for power-law fluids, as follows:

$$\eta_{app} = Be^{\frac{E_\gamma}{RT}} \quad (12)$$

where E_γ is the activation energy of the flow at a particular shear rate, R is the universal gas constant, T is the temperature (K), B is the pre-exponential component, and η_{app} is the apparent shear viscosity (kPa s) at a particular shear rate. The value of E_γ/R was obtained from the slope of a linear plot of the logarithm of the viscosity versus the reciprocal of the temperature ($1/T$), which was used to calculate the activation energy. To determine the activation energy, studies were carried out at three different temperatures (120, 130, and 140°C).

Scanning electron microscopy (SEM) studies and energy-dispersive X-ray mapping (EDX)

The surface morphology of the extrudate profile was studied with a JEOL JSM-5800 (JEOL Ltd., Tokyo, Japan) scanning electron microscope operating at an accelerating voltage of 20 kV. A 2–3-mm-long extrudate sample was mounted on a stub with carbon tape. After that, the stub was placed on a holder. The samples were sputter-coated with gold before the SEM analysis. Finally, the holder was placed inside the machine chamber for analysis. The X-ray sulfur mapping of the gel-filled raw rubber systems was recorded with an Oxford EDX (Oxford Instrument, Oxfordshire, United Kingdom) system attached to the scanning electron microscope.

RESULTS AND DISCUSSION

Characterization of the sulfur-crosslinked NR latex gel

Raw NR latex was vulcanized by sulfur in the presence of ZDC as an accelerator and ZnO as an accelerator activator. The sulfur-to-accelerator ratios were kept at 3, 2, 1, 0.5, and 0.33 (Table I).

Variation in the gel content and crosslink density with the sulfur-to-accelerator ratio

The values of the gel content and crosslink density of the various gels used in this study are reported in Table II. The gel content increases with a higher concentration of sulfur, from 86% in $NS_{0.33}$ to 94% in NS_1 and 97% in NS_3. The increase in the gel content with the increasing sulfur dose is due to the formation of a three-dimensional network structure initiated by sulfide linkages. At a higher sulfur loading, the increase in the gel content is marginal because of the saturation of sites available for crosslinking. An increase in the sulfur-to-accelerator ratio also results in a higher value of the crosslink density, as is evident from Table II, for a reason similar to that stated previously. NS_3 gives the highest value of the crosslink density as it has the maximum amount of sulfur.

DLS studies

DLS was used to determine the particle size and particle size distribution of the gel particles. Figure 1

TABLE II
Properties of the Various Gels

Gel type	Gel content (%)	Crosslink density (kmol/m^3)	Z_{avg} diameter (nm)	Tensile strength (MPa)	Elongation at break (%)
$NS_{0.33}$	86	0.27	—	12.00	1220
$NS_{0.5}$	88	0.36	205	12.70	1200
NS_1	94	0.75	219	15.80	1170
NS_2	96	1.00	214	17.00	1125
NS_3	97	1.11	—	18.90	1120

depicts the distribution of the particle diameters for raw NR and various prevulcanized latex gels. It reveals a narrower distribution of particle sizes for all the systems studied, with a size range of 122–295 nm, which is well within the size range reported in the literature.[22] Because part of the distribution of the size scale of the gels swings close to the nano-range of 100 nm, these can be termed quasi-nanoparticles. The values of Z_{avg} the mean hydrodynamic particle diameter, are (nm) for various gels are listed in Table II. However, the particle diameter is around 200 nm for the investigated systems (cf. 214 nm for NS_2 and 220 nm for N_0). Thus, the particle size distribution and individual particle sizes remain approximately unaltered after the sulfur prevulcanization of the NR latex.

Tensile properties

Table II also summarizes the tensile properties of the various sulfur-prevulcanized latex gels used in this study. It is quite clear that the tensile strength of the various gelled latexes increases steadily with their increasing crosslink densities and is highest for NS_3. The elongation at break decreases steadily with an increasing crosslink density and is lowest for NS_3, as expected. The reduction in the elongation at break is due to the restriction imparted by a greater number of interchain sulfide crosslinks.

Rheological behavior of gel-mixed raw NR

Effect of the gel on the raw NR viscosity

Plots of η_{app} versus $\dot{\gamma}_{app}$ on logarithmic scales for raw NR filled with three representative sulfur-crosslinked gels ($NS_{0.5}$, NS_1, and NS_2) at 130°C are shown in Figure 2(a–c). The viscosity decreases with an increase in the shear rate, and this shows the pseudoplastic or shear-thinning behavior of all the systems studied. All elastomers are known to behave in a similar fashion, and some of the recent publications from our laboratory vindicate this behavior of rubbers with capillary rheometry studies.[13,14] Interestingly, in Figure 2(a,b), with $NS_{0.5}$ (sulfur-to-accelerator ratio of 0.5) and NS_1 (sulfur-to-accelerator ratio of 1) gels, the viscosities of the gel-filled raw rubbers are considerably lower, especially at lower shear rates, than those of the unfilled raw NR. The system containing $NS_{0.33}$ behaves in a similar fashion. However, the raw NR filled with NS_2 gels (sulfur-to-accelerator ratio of 2) shows a marginal reduction in the melt viscosity [Fig. 2(c)]. In the case of NS_3 gels (not shown here), the scenario changes completely. It conceivably behaves like any other rigid particulate inclusions, and the viscosity of these gel-filled samples is much higher than that of the control. The variation in the viscosity with the gel loading is plotted in Figure 3 for all five types of gel systems at a representative shear rate and temperature. For $NS_{0.5}$ and NS_1, even with the addition of 2 phr gel, the raw rubber viscosity decreases considerably and further decreases up to a 8 phr gel loading. After that, the viscosity starts to rise sharply with the addition of the gel (16 phr), but it never crosses the unfilled raw NR value (N_0). However, as stated earlier for the NS_2 gel, the gel-filled raw NR has a viscosity similar to that of the unfilled raw NR. In this case, η_{app} of $NS_{2/16}$ is approximately equal to that of $N_{0/0}$. Hence, both the NS_3 and NS_2 gels exhibit a reversal of the trend of the other three types.

Normally, the addition of a rigid particulate filler or a gel to a raw polymer matrix leads to an increase in its melt viscosity because of the greater resistance

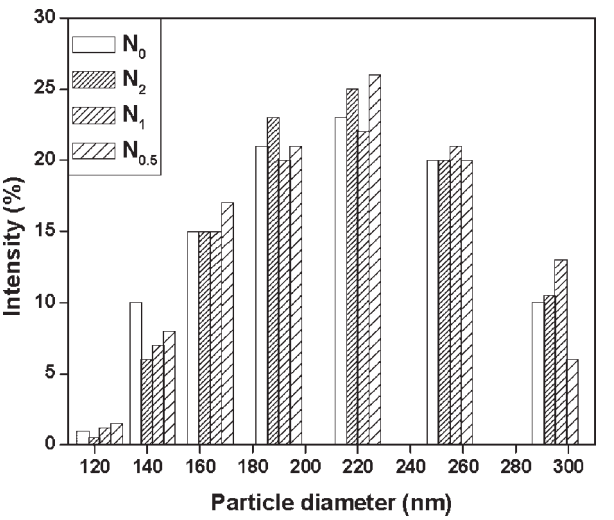

Figure 1 Particle size distributions of different gels as determined by the DLS method.

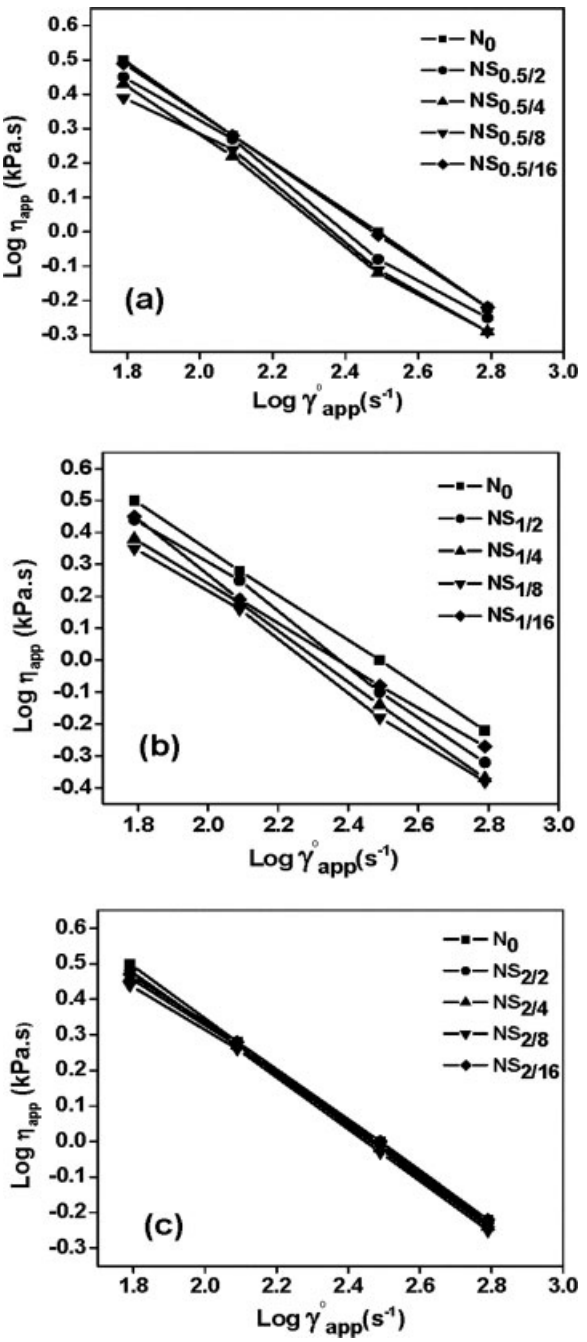

Figure 2 Log–log plot of η_{app} versus $\dot{\gamma}_{app}$ for different gel-filled systems with (a) $NS_{0.5}$, (b) NS_1, and (c) NS_2 gels.

that they offer to flow,[8,23,24] with a few exceptions.[7,13,20] In this case, probably the large polymer chains roll over or slip past the comparatively semirigid, quasi-nanogel particles, and this leads to a substantial decrease in the melt viscosity at an intermediate shear rate. This can be attributed to the relatively large flow unit of the uncrosslinked polymer chains in comparison with the quasi-nanosized gel particles.[7] As the gel loading increases beyond 8 phr, the viscosity again starts to rise, and this indicates additional resistance to flow due to the contribution

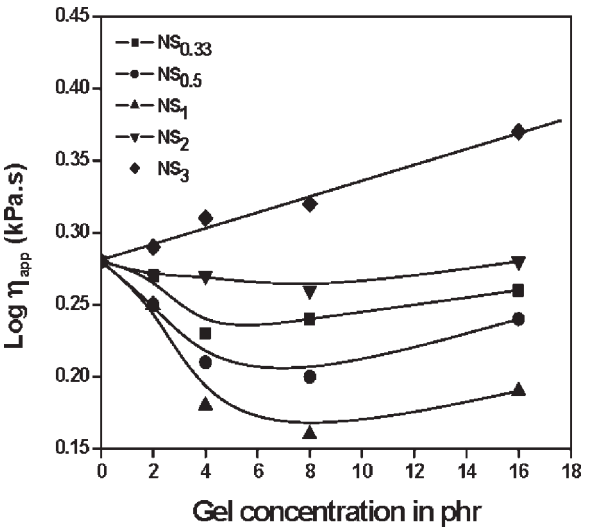

Figure 3 Variation in η_{app} of sulfur-prevulcanized latex gel-filled systems with the gel loading at 130°C and a shear rate of 122.5 s^{-1}.

of the viscoelastic relaxation of quasi-nanogel agglomerates. This behavior of the gel particles seems to be dependent on their crosslink densities. The dependence of the viscosity on the crosslink densities of the added gels at an 8 phr concentration and a 122.5-s^{-1} shear rate is shown in Figure 4. As the crosslink density of the gel particles increases, it becomes more effective in reducing the viscosity of the raw matrix. However, after a critical crosslink density value is passed, the addition of gels actually increases the viscosity of the raw matrix (for NS_3). This can be related to the rigidity of the gel particles. Gels having lower crosslink densities are easily deformable and require less energy to flow, and flow units can slip past them comfortably. With increasing crosslink densities, they

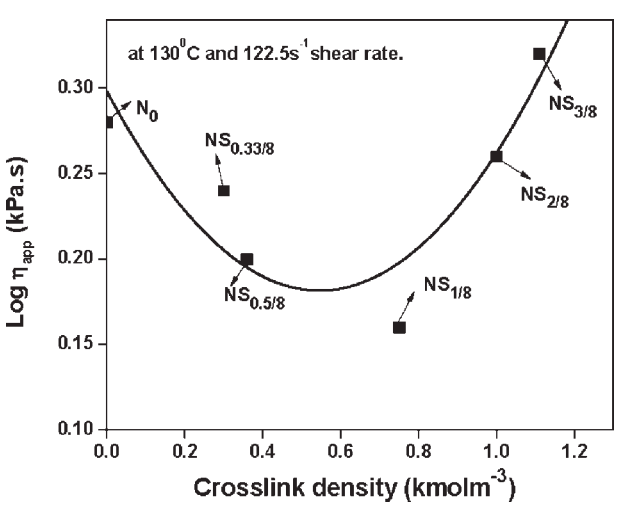

Figure 4 Variation in η_{app} with the crosslink density of the gel with an 8 phr gel loading at 130°C and a shear rate of 122.5 s^{-1}.

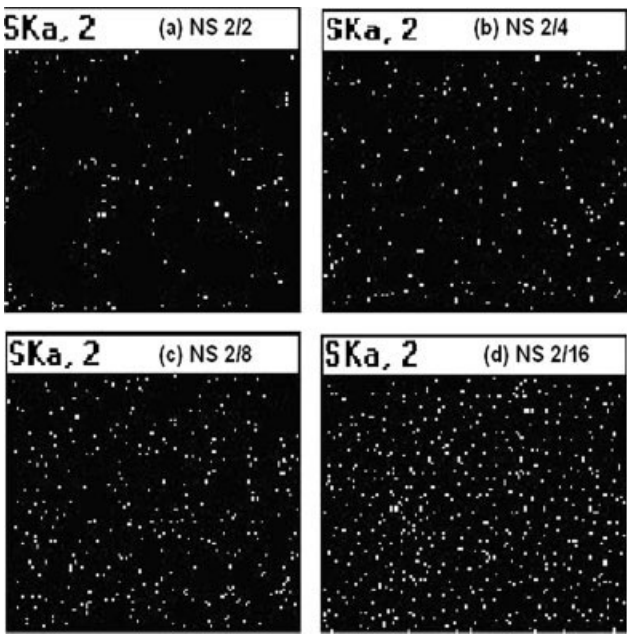

Figure 5 X-ray sulfur dot mapping of different gel-filled samples by EDX for (a) $NS_{2/2}$, (b) $NS_{2/4}$, (c) $NS_{2/8}$, and (d) $NS_{2/16}$ systems.

become more rigid, more like a particulate filler that is not at all deformable, and they start to offer resistance to flow. This has been substantiated as follows. To check the dispersion of the gel particles into the raw NR matrix, EDX of sulfur was carried out. Figure 5(a–d) presents representative EDX pictures of raw NR containing 2, 4, 8, or 16 phr NS_2 gel, respectively. It is evident that the gels are uniformly distributed into the raw NR matrix. As the concentration of the gel increases beyond 8 phr, the quasi-nanogel particles start to show some sign of aggregation. This type of aggregation offers greater resistance to flow. This explains the cause of the sudden increase in the melt viscosity beyond an 8 phr gel loading in all the systems studied.

Various properties of the composites, such as the viscosity and mechanical properties, are affected by a number of factors, including the size, shape, aspect ratio, and distribution of the particulate inclusions. The viscosity of such composite systems can be expressed by the following relation, which is derived from Einstein's[25] equation for the viscosity of a suspension of rigid spherical inclusions:

$$\eta_c = \eta_m(1 + K_E V_P) \tag{13}$$

where η_c and η_m are the viscosities of the suspension and matrix, respectively. K_E is equal to 2.5 for spherical particles, and V_P is the volume fraction of the particulate inclusions. This equation was modified later to express the changes in the modulus when particulate fillers are introduced into a polymer matrix. Guth[26] introduced the particle interaction term and adapted the equation into the following form:

$$G_c = G_m(1 + 2.5V_P + 14.1V_P^2) \tag{14}$$

where G_c and G_m are the shear moduli of the composite and matrix, respectively. When this equation was derived, it was assumed that $\eta_c/\eta_m = G_c/G_m$.[27] Therefore, the Guth equation should also hold for the changes in the viscosity. Therefore, the equation can be rewritten in terms of the viscosity:

$$\eta_c = \eta_m(1 + 2.5V_P + 14.1V_P^2) \tag{15}$$

where 2.5 is Einstein's coefficient for spherically shaped particles. However, for nonspherical particulate inclusions, a modified equation has been proposed:

$$\eta_c = \eta_m(1 + 0.67\psi V_P + 1.62\psi^2 V_P^2) \tag{16}$$

where ψ is a factor related to the shape of the particulate fillers. It is defined as the ratio of the particle length to width. In the case of fillers, the particulate inclusions are essentially considered rigid inclusions that have a modulus difference of a few decades from the virgin matrix. For example, carbon black has a Young's modulus of 1.0 GPa,[28] and that of dickite clay is around 6.20 GPa,[12] as measured with the help of atomic force microscopy, whereas the modulus of an elastomer matrix ranges from ~ 0.5 to ~ 20 MPa in most cases. However, in the case of the present systems, sulfur-crosslinked gels have been used that are partially deformable, and their moduli can be marginally higher than that of the virgin polymer. For such particulate inclusions, which are at most semirigid, the following modification for the Guth equation is proposed:

$$\eta_c = \eta_m(1 + 2.5aV_g + 14.1bV_g^2) \tag{17}$$

where a and b are two coefficients that are assumed to be functions of the crosslink density of the gels used (discussed later) and V_g is the volume fraction of the added gel. The gel particles are also essentially taken to be spherical in shape, and these exist in the matrix, forming well-defined interfaces. Figure 6 shows the polynomial fitting plot of all the systems. The values of a and b were calculated from the polynomial fitting plots of η_{app} versus the volume fraction of the gel for the different systems with OriginPro 7.5 software (Origin Lab Corporation, Northampton, MA) and a 95% confidence limit. In all cases, the value of the regression coefficient was greater than 0.98. In Table III, the values of η_m, a, and b are listed for all the systems studied. The NS_3 gel causes an increase in the raw NR viscosity, much as a conventional rigid particulate filler reinforcement would. However, at a lower crosslink density of the gel, η_{app} first decreases and then increases at a higher gel concentration.

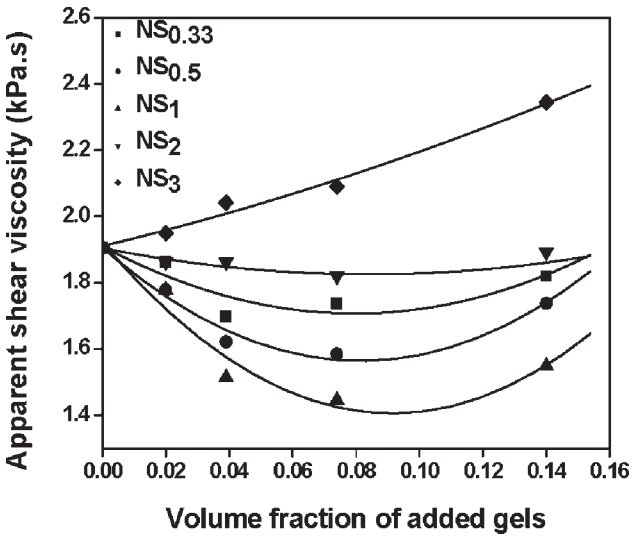

Figure 6 Polynomial fitting curve of the apparent viscosity versus the volume fraction of the gel-filled for different gel systems.

Up to a sulfur-to-accelerator ratio of 2.0, the absolute values of coefficients a and b are comparable. Therefore, the viscosity expression [eq. (17)] for them can be reduced to the following form:

$$\eta_c = \eta_m(1 + 2.5aV_g + 14.1aV_g^2) \tag{18}$$

The numerical value of a decreases steadily with an increasing sulfur-to-accelerator ratio and passes through a minimum for the NS_1 gel system. After that, it increases again and becomes positive for the NS_3 gel system. On the other hand, b reaches a maximum for NS_1 before a decrease. It seems that the crosslink density of NS_1, which is around 0.75 kmol/m^3, is very critical, in that it reduces the viscosity of the raw NR considerably. Probably up to this value of the crosslink density, the gels remain deformable enough to allow slippage of flow units, which facilitates the lowering of the viscosity. However, as the crosslink density increases, the gels become more and more rigid and less deformable, thus behaving like conventional particulate reinforcement; this is manifested in the rise in the viscosity of the NS_3-gel-filled raw NR systems. At a sulfur-to-accelerator ratio of 3, the numerical values of coefficients a and b become positive. Thus, following these trends, we can quite rationally expect that after a critical crosslink density, the viscosity relation will conform to the Einstein–Guth equation [eq. (15)]; that is, the numerical values of a and b will be unity. It is worth mentioning at this stage that the preparation of gels in the latex stage at a sulfur-to-accelerator ratio higher than 3 is extremely difficult as the particles starts depositing from the latex stage at a higher sulfur-to-accelerator ratio. The coefficients a and b are functions of the crosslink density and can be expressed as follows:

$$a = 2.2 - 154X + 1260X^2 \tag{19}$$

$$b = e^{(127X - 1102\ X^2 - 2.5)} \tag{20}$$

where X is the crosslink density of the gels (kmol/m^3).

The flow behavior of raw NR with and without gels is quite well represented by the power-law model. The power-law constants n' and k have been calculated from the linear fit of the curves of the viscosity versus the shear rate for representative $NS_{0.5}$, NS_1, and NS_2 systems and are tabulated in Table IV. The k values decrease with an increase in the gel loading up to 8 phr, beyond which they increase. This indicates that the resistance to flow for the gel-filled raw rubber system is much less than that for the unfilled raw rubber and the 16 phr gel loaded samples for the $NS_{0.5}$ and NS_1 types of gels. In the case of NS_2-gel-filled systems, the k value is very close to that of N_0. The reason for this has already been stated. The variation in n' is marginal, and it shows pseudoplastic behavior ($n' < 1$) for raw NR and gel-filled raw NR systems. The value lies within 0.29–0.33 and does not follow any particular trend.

TABLE III
Curve-Fitting Values of η_m, a, and b

Gel systems	η_m (kPa s)	a	b
$NS_{0.33}$	1.91	−1.07	1.19
$NS_{0.50}$	1.91	−1.76	1.92
NS_1	1.92	−2.35	2.28
NS_2	1.90	−0.40	0.42
NS_3	1.91	0.48	0.20

Effect of the gel on the die swell of the raw rubber

Figure 7(a–c) exhibits the variation in the die swell with the experimental shear rates at 130°C for three representative gel systems. Because of the unfilled and raw nature of the NR and its high molecular

TABLE IV
Values of n' and k at 130°C

Sample	k ($\times 10^{-3}$ kPa s^n)	n'
N_0	60.70	0.31
$NS_{0.5/2}$	52.20	0.33
$NS_{0.5/4}$	48.70	0.31
$NS_{0.5/8}$	46.80	0.29
$NS_{0.5/16}$	50.30	0.30
$NS_{1/2}$	42.30	0.31
$NS_{1/4}$	39.80	0.30
$NS_{1/8}$	36.30	0.32
$NS_{1/16}$	43.10	0.33
$NS_{2/2}$	58.20	0.32
$NS_{2/4}$	57.30	0.31
$NS_{2/8}$	57.80	0.31
$NS_{2/16}$	60.80	0.30

weight, all the systems including the raw NR show large values of the die swell.[14] The die swell increases almost linearly with the experimental shear rate. For example, N_0 has a die swell value of 118% at a 61.3-s^{-1} shear rate, which increases up to 137% at 612.5 s^{-1}. However, as expected, the introduction of a small concentration of a crosslinked gel into the raw NR matrix reduces the die swell to a great extent. For any given shear rate, the die swell values of 16 phr gel-filled NR are at least 10% lower than those of unfilled raw NR (e.g., $NS_{2/16}$ and $NS_{1/16}$ vs N_0). Unlike the viscosity, the die swell decreases exponentially with the increase in the gel loading within the experimental range at a representative shear rate of 122.5 s^{-1}, as is evident from Figure 8. In this case, gels having a higher crosslink density (e.g., NS_2 and NS_3) seem to be more effective in reducing the die swell than their counterparts. Thus, it has been clearly demonstrated here that both the die swell and viscosity can be monitored and manipulated by the variation of the crosslink density of the gel.

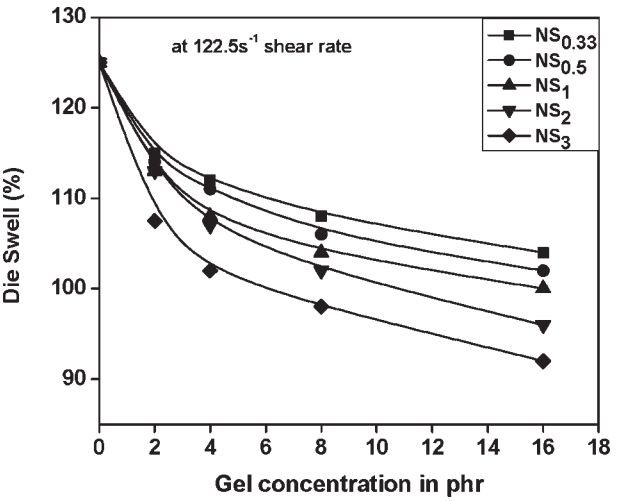

Figure 8 Effects of the sulfur-crosslinked gel loading on the die swell property of raw NR.

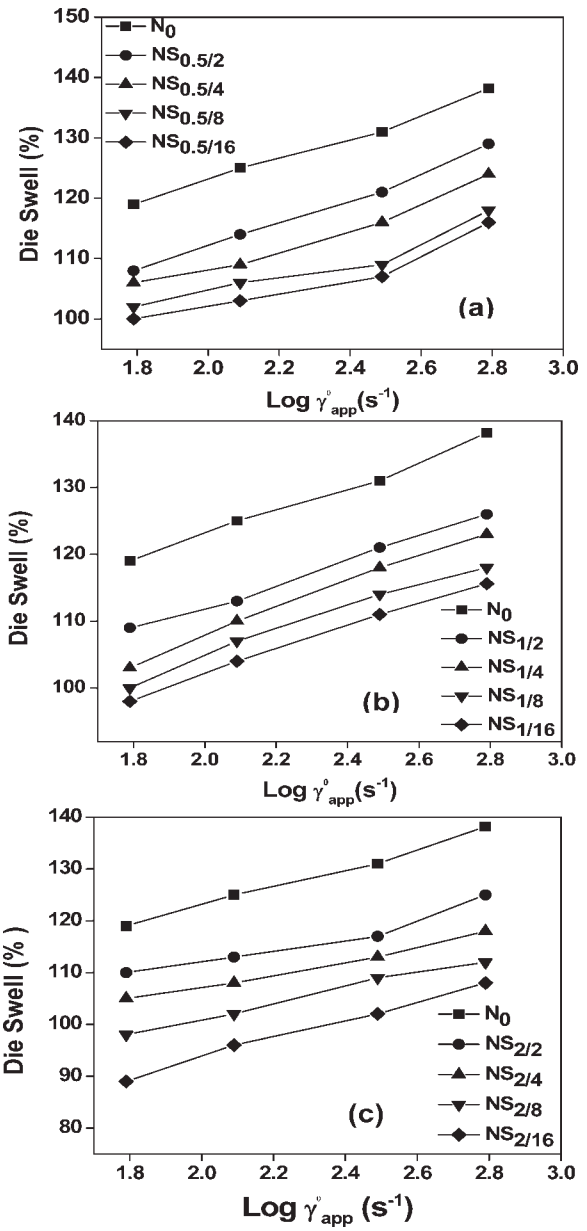

Figure 7 Plot of the die swell versus log $\dot{\gamma}_{app}$ for different gel-filled systems with (a) $NS_{0.5}$, (b) NS_1, and (c) NS_2 gels.

The die swell is the manifestation of the recovery of the elastic deformation imposed during the flow through the capillary.[19] The decrease in the die swell indicates the more viscous nature of the material, whereas the higher value of the same represents the contribution of the elastic component. The predominant viscous or elastic effect within the experimental shear rate is fully influenced by the nature of the polymer, as it controls the level of normal stress generated within the barrel and the die region of the processing instrument. To understand the elastic effect within these systems more distinctively, the first normal stress difference has been calculated within the experimental shear rates with eq. (22) at 130°C. The logarithmic value for the representative NS_1 system of the normal stress difference, when plotted against log τ_{app}, gives a straight line, as shown in Figure 9:

$$\sigma_E = I(\tau_{app})^m \tag{21}$$

or

$$\log \sigma_E = \log(I) + m \log(\tau_{app}) \tag{22}$$

The slope (m) and intercept (log I) values calculated with the best fit line (with a 97% confidence limit) are tabulated in Table V for the $NS_{0.5}$, NS_1, and NS_2 systems. The value of m increases and I decreases at

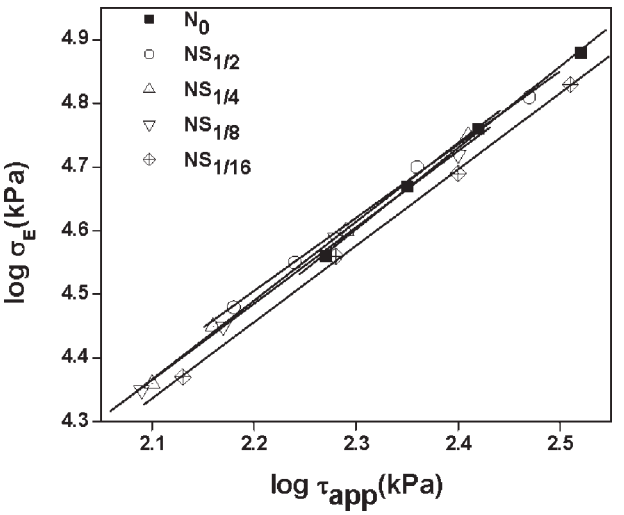

Figure 9 Plot of log σ_E versus log τ_{app} for the control and NS_1 system.

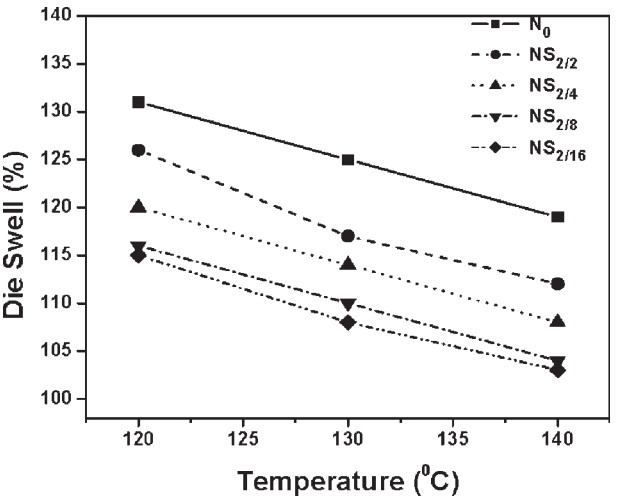

Figure 10 Temperature dependence of the die swell for the NS_2 system.

130°C for the gel-filled raw NR versus the control raw NR sample. This is primarily due to the incorporation of crosslinked gel particles into the raw rubber, which reduces the elastic (memory) effect in the raw rubber by enhancing the viscous nature of the raw rubber matrix. At the same time, because of the rollover or slip effect of these gels, gel-filled polymer chains experience less elastic strain than their unfilled counterparts, and this facilitates bringing down the die swell value. This lowering of the elastic strain[29] contributes to the overall improvement in the processability of raw NR.

Effect of the temperature on the die swell

The die swell of both raw NR and gel-filled raw NR systems decreases to a great extent with a progressive increase in the temperature (Fig. 10). The reduction in the die swell is greater in the case of raw NR than the NS_2-gel-filled systems at the representative shear rate of 122.5 s^{-1}. The decrease is more evident at a higher temperature (140°C). The reduction in the die swell values with increasing temperature has been reported in the literature.[18] Unfilled raw NR can store more elastic energy because of the higher chain entanglements. This effect decreases sharply with an increase in the temperature. This is due to the greater mobility imparted to the polymer chains with higher thermal energy, which leads to a progressive reduction in the maximum relaxation time for flow. In the case of the gel-filled raw NR systems, the more viscous nature of the crosslinked gels (evident from Table V) probably restricts extensive chain uncoiling during the flow through the capillary and as a result gives rise to lower die swell values.

TABLE V
***m* and Log *I* Values of the Raw NR and Gel-Filled NR Samples at 130°C**

Sample	*m*	Log *I*
N_0	0.45	3.54
$NS_{0.5/2}$	0.46	3.52
$NS_{0.5/4}$	0.47	3.51
$NS_{0.5/8}$	0.47	3.51
$NS_{0.5/16}$	0.48	3.47
$NS_{1/2}$	0.46	3.50
$NS_{1/4}$	0.47	3.48
$NS_{1/8}$	0.47	3.48
$NS_{1/16}$	0.49	3.45
$NS_{2/2}$	0.47	3.50
$NS_{2/4}$	0.49	3.43
$NS_{2/8}$	0.50	3.40
$NS_{2/16}$	0.53	3.38

Effect of the gel on the extrudate roughness

Figure 11(a–e) shows SEM photomicrographs of the extrudates of raw NR and NS_1-gel-filled systems at a representative shear rate of 122.5 s^{-1} taken at a magnification of 35×. It is quite clear from the SEM photomicrographs that as the concentration of the gel in the raw rubber increases, its surface roughness improves tremendously. The raw NR shows a maximum amount of die swell and provides a very rough, irregular, and rippled extrudate surface that is due to the elastic effect or melt fracture observed in various high-molecular-weight polymers. Melt fracture is the manifestation of the normal stress generated during extrusion through the capillary. Compared with N_0, $NS_{2/2}$ and $N_{2/4}$ exhibit much reduced surface roughness; however, $NS_{2/8}$ and $NS_{2/16}$ show even smoother extrudate surfaces with almost no sign of any melt fracture. Similar trends have been observed in all the other systems. For any given system, the extrudate

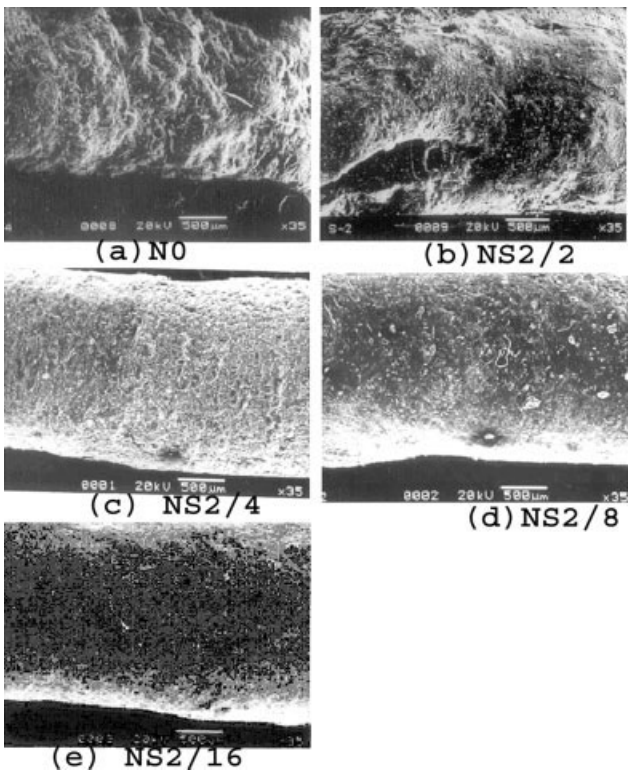

Figure 11 SEM photomicrographs of extrudates for (a) N_0, (b) $NS_{2/2}$, (c) $NS_{2/4}$, (d) $NS_{2/8}$, and (e) $NS_{2/16}$.

roughness increases with an increasing shear rate, and this indicates a higher elastic memory effect. The incorporation of a crosslinked gel into raw rubber reduces the first normal stress difference values (as given in Table IV), and this leads to the lowering of the die swell values and consequently leads to a smoother extrudate surface.

Activation energy of the melt flow

The dependence of the activation energy and shear rates is plotted in Figure 12 for representative raw NR samples containing the NS_1 type of gel. In all cases, as expected, the activation energy decreases with an increase in the shear rate within the experimental range of shear rates. The activation energy of raw NR at any particular shear rate is actually higher than that of gel-filled raw NR, as shown here for the NS_1 gel system (Fig. 12). For example, at a 122.5-s^{-1} shear rate, N_0 has an activation energy value of 18 kJ/mol versus 10 kJ/mol for $NS_{1/8}$. The activation energy decreases with the gel loading up to 8 phr and then starts to increase. This observation is in line with the trend of the apparent viscosity variation with the gel loading, as stated earlier, and therefore can be explained with similar reasoning. For all cases, the drop in the activation energy value at lower shear rates is very sharp, and they tend to level off at comparatively higher shear rates.

Effect of the gel on the mechanical properties of raw NR

The effect of the sulfur-crosslinked gels on the tensile strength, modulus at 5% elongation, and elongation at break of raw NR has been studied. The values are tabulated in Table VI. It is quite clear that the incorporation of a sulfur-crosslinked gel into the raw rubber matrix increases the tensile strength and modulus with an accompanying decrease in the elongation at break. For example, gels having a higher crosslink density produce greater strength in the mixed system $NS_{2/16}$ (cf. $N_{0.5/16}$). The tensile strength versus the crosslink density of the gels is plotted in Figure 13, which shows that the tensile strength increases steadily with the crosslink density and with the increasing concentration of the gels. The tensile strength of $NS_{3/16}$ (3.86 MPa) is more than double that of N_0 (1.85 MPa). As the crosslinked gels having higher tensile strengths and moduli are introduced into the raw rubber, the tensile strength and modulus of the systems rise, depending on the corresponding properties of the respective gels. The moderate decrease in the elongation at break with the increase in the gel loading is due to the restricted mobility of the chains under tensile forces in the presence of the crosslinked gels. The 5% modulus values are very important for understanding the effect of the gel on the tensile properties of raw rubber. The 5% modulus increases steadily with an increasing gel loading. This is due to the higher resistance to tensile deformation provided by

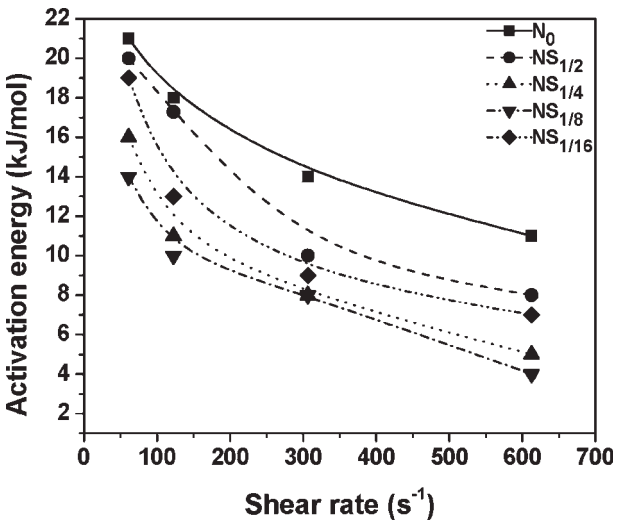

Figure 12 Plot of the activation energy versus the shear rate for the NS_1 system.

TABLE VI
Tensile Properties of Different Gel-Filled Raw NR Samples

Sample	Tensile strength (MPa)	Elongation at break (%)	Modulus at 5% elongation (MPa)
N_0	1.85 ± 0.05	1400 ± 15	0.04 ± 0.01
$NS_{0.33/2}$	1.99 ± 0.02	1385 ± 10	0.04 ± 0.01
$NS_{0.33/4}$	2.20 ± 0.02	1375 ± 10	0.05 ± 0.01
$NS_{0.33/8}$	2.75 ± 0.05	1345 ± 10	0.06 ± 0.01
$NS_{0.33/16}$	3.00 ± 0.03	1305 ± 5	0.06 ± 0.01
$NS_{0.5/2}$	2.00 ± 0.04	1390 ± 15	0.05 ± 0.01
$NS_{0.5/4}$	2.25 ± 0.06	1370 ± 10	0.06 ± 0.01
$NS_{0.5/8}$	2.81 ± 0.04	1330 ± 5	0.06 ± 0.01
$NS_{0.5/16}$	3.05 ± 0.03	1300 ± 15	0.07 ± 0.01
$NS_{1/2}$	2.05 ± 0.02	1370 ± 10	0.06 ± 0.02
$NS_{1/4}$	2.35 ± 0.05	1350 ± 10	0.08 ± 0.02
$NS_{1/8}$	2.90 ± 0.04	1300 ± 5	0.10 ± 0.02
$NS_{1/16}$	3.30 ± 0.03	1280 ± 10	0.11 ± 0.02
$NS_{2/2}$	2.15 ± 0.02	1320 ± 5	0.08 ± 0.02
$NS_{2/4}$	2.70 ± 0.04	1270 ± 10	0.09 ± 0.02
$NS_{2/8}$	3.25 ± 0.02	1240 ± 10	0.11 ± 0.02
$NS_{2/16}$	3.65 ± 0.10	1220 ± 5	0.12 ± 0.02
$NS_{3/2}$	2.35 ± 0.02	1280 ± 10	0.08 ± 0.02
$NS_{3/4}$	3.05 ± 0.03	1240 ± 10	0.10 ± 0.01
$NS_{3/8}$	3.50 ± 0.02	1235 ± 5	0.12 ± 0.02
$NS_{3/16}$	3.86 ± 0.05	1220 ± 5	0.13 ± 0.01

the network structure of the gels, which is very pronounced at a low strain level.

Effect of the gel on the dynamic mechanical properties of raw NR

Dynamic mechanical thermal analysis plots, that is, plots of the storage modulus and tan δ versus the temperature, for representative samples (the N_0, $NS_{2/4}$, $NS_{2/8}$, and $NS_{2/16}$ systems) are shown in Figure 14. Raw NR (N_0) has a storage modulus value of 324 MPa at −80°C; these values are 2187 MPa for 4 phr and 3235 MPa for 8 phr for the raw NR containing NS_2 gel. The storage modulus increases with increasing gel content. This follows the same trend of the low-strain static modulus described earlier. Similar results have been obtained for the other systems at various gel concentrations. As the temperature is increased, the modulus decreases sharply near the glass-transition temperature, beyond which it remains almost constant. At 30°C, the storage modulus values are quite low: 0.22 MPa for N_0 and 0.95 MPa for $NS_{2/8}$. However, as the gel loading in the matrix increases, the peak tan δ_{max} value decreases (given as an inset in Fig. 14). The tan δ curve is also broadened, and its peak height decreases gradually with the addition of 4 and 8 phr NS_2 gel to the raw NR matrix. The peak tan δ value

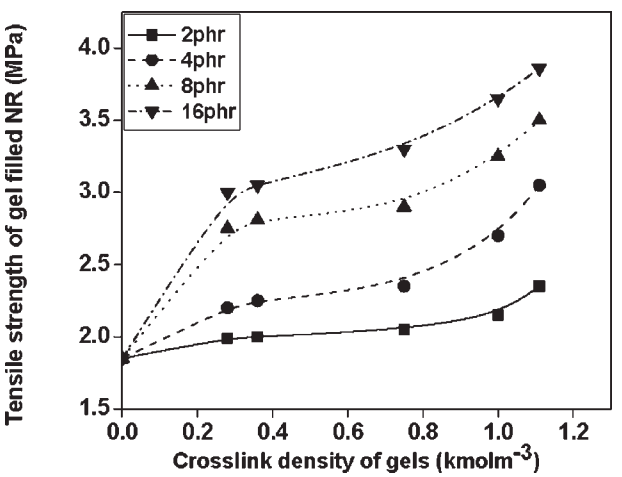

Figure 13 Variation of the tensile strength of the gel-filled systems with the crosslink densities of the respective gels.

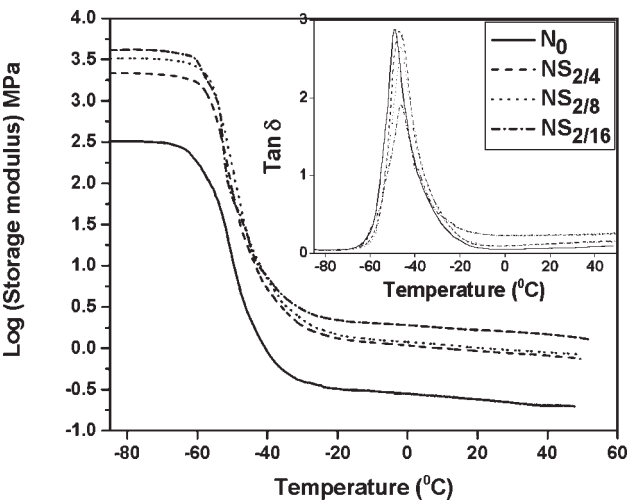

Figure 14 Temperature variation of the storage modulus and tan δ plots (inset) for the control and gel-filled raw NR.

for N_0 is 2.88, whereas it is 2.67 for $NS_{2/8}$ and 1.94 for the $NS_{2/16}$ system. The temperature at which the peak maximum occurs shifts toward a higher value ($-49.0^\circ C$ in N_0 to $-46.2^\circ C$ in $NS_{2/16}$) because of the restricted mobility imparted by the crosslinked gel particles. The presence of crosslinks in the raw NR matrix hinders the segmental motions of the polymer chains; therefore, the glass-transition temperature is shifted to a higher temperature. Similarly, the increase in the storage modulus upon the gel loading is manifested by the greater resistance to deformation imparted by the crosslinked network.

CONCLUSIONS

In this research, sulfur-crosslinked, quasi-nanosized NR latex gels were prepared and characterized with various methods. The rheological, mechanical, and dynamic mechanical properties of the raw NR and NR containing sulfur-crosslinked, quasi-nanogels were investigated. On the basis of this study, the following conclusions have been drawn.

η_{app} of raw NR and quasi-nanogel filled raw NR systems decreases with an increase in the shear rate, showing shear-thinning or pseudoplastic behavior. These quasi-nanogels affect the shear viscosity in different ways according to their nature and crosslink densities. Deformable gels with a low crosslink density drastically reduce the viscosity of raw NR up to an optimum loading of 8 phr. However, comparatively rigid gels with higher crosslink densities are not effective in reducing the viscosity. They behave like conventional rigid particulate reinforcements, increasing η_m. This anomaly has been explained with the help of an empirical relation between the viscosity and crosslink density of the gels.

The sulfur-crosslinked gels also improve the die swell of raw NR to a marked extent. The die swell decreases steadily with an increase in the gel loading, and more than a 10% reduction in the die swell is obtained with a gel loading as low as 4 phr. This is explained by the calculation of the normal stress difference for all the systems. The first normal stress difference values decrease steadily with the gel loading. The reduction in the die swell is also due to the lesser amount of elastic strain experienced by the polymer chains. The surface smoothness of the gel-filled raw NR extrudates becomes progressively better with an increasing gel loading, as revealed by SEM photomicrographs.

The tensile strength and modulus of the gel-filled rubbers are improved compared with those of the pristine ones, and the extent of the improvement depends on the tensile strength and modulus of the gels used. However, the elongation at break decreases consistently upon gel loading. The storage modulus of the gel-filled systems also substantiates this. The maximum of the tan δ curve shows a marginal shift toward a higher temperature with the gel loading.

The authors sincerely acknowledge the help of Rosamma Alex of the Rubber Research Institute of India. They are also thankful to Suman Roy of Aimil, Ltd., and Ashish Bhattacharya and Syed Mustaq for their assistance and help with the dynamic light scattering and rheological studies, respectively.

References

1. Fahrlander, M.; Bruch, M.; Menke, T.; Friedrich, C. Rheol Acta 2001, 40, 1.
2. Li, J. Q.; Salovey, R. Polym Eng Sci 2004, 44, 452.
3. Bousmina, M.; Muller, R. J Rheol 1993, 37, 663.
4. Bischoff, A.; Kluppel, M.; Schuster, R. H. Polym Bull 1998, 40, 283.
5. Kluppel, M.; Schuster, R. H.; Heinrich, G. Rubber Chem Technol 1997, 70, 243.
6. Hofman, W. Rubber Chem Technol 1964, 37, 85.
7. Nakajima, N.; Collins, E. A. J Rheol 1978, 22, 547.
8. Montes, S. A.; Ponce-Velez, M. A. Rubber Chem Technol 1983, 56, 1.
9. Bhowmick, A. K.; Cho, J.; MacArthur, A.; McIntyre, D. Polymer 1986, 27, 1889.
10. Campbell, D. S.; Fuller, K. N. G. Rubber Chem Technol 1984, 57, 104.
11. Kawahara, S.; Isono, Y.; Sakdapipanich, J. T.; Tanaka, Y.; Aik-Hwee, E. Rubber Chem Technol 2002, 75, 739.
12. Prasad, M.; Kopycinska, M.; Rabe, U.; Arnold, W. Geophys Res Lett 2002, 29, 1172.
13. Sadhu, S.; Bhowmick, A. K. J Polym Sci Part B: Polym Phys 2005, 43, 1854.
14. Bandyopdhyay, A.; DeSarkar, M.; Bhowmick, A. K. Rubber Chem Technol 2005, 78, 806.
15. Claramma, N. M.; Mathew, N. M. J Appl Polym Sci 1997, 65, 1913.
16. Sperling, L. H. Introduction to Physical Polymer Science, 2nd ed.; Wiley: New York, 1992; p 429.
17. Bhowmick, A. K.; Mangaraj, D. In Rubber Products Manufacturing Technology; Bhowmick, A. K.; Hall, M. M.; Benarey, H., Eds.; Marcel Dekker: New York, 1994; p 385.
18. Shanmugharaj, A. M.; Bhowmick, A. K. Radiat Phys Chem 2004, 61, 91.
19. Brydson, J. A. Flow Properties of Polymer Melts, 2nd ed.; George Godwin: London, 1981; p 17.
20. Kumar, N. R.; Bhowmick, A. K.; Gupta, B. R. Kautsch Gummi Kunstst 1992, 45, 531.
21. Vinogradov, G. V.; Ya Malkin, A. Rheology of Polymers; Mir: Moscow, 1979; pp 106 and 304.
22. Sanguansap, K.; Suteewong, T.; Saendee, P.; Buranabunya, U.; Tangboriboonra, P. Polymer 2005, 46, 1373.
23. Leblanc, J. L. Prog Polym Sci 2002, 27, 627.
24. Kumar, B.; De, S. K.; Bhowmick, A. K.; De, P. P. Polym Eng Sci 2002, 42, 2306.
25. Einstein, A. Investigation on Theory of Brownian Motion; Dover: New York, 1956.
26. Guth, E. J Appl Phys 1951, 16, 21.
27. Ahmed, S.; Jones, F. R. J Mater Sci 1990, 25, 4933.
28. Nishi, T.; Nukaga, H.; Fujinami, S.; Nakajima, K. Chin J Polym Sci 2007, 25, 35.
29. Rosen, S. L.; Rodriguez, F. J Appl Polym Sci 1965, 9, 1615.